A fish scale–derived collagen matrix as artificial cornea in rats: properties and potential

Essen, T.H. van; Lin, C.C.; Hussain, A.K.; Maas, S.; Lai, H.J.; Linnartz, H.V.J.; ... ; Jager, M.J.

A Fish Scale–Derived Collagen Matrix as Artificial Cornea in Rats: Properties and Potential

T. Huibertus van Essen,[1] Chien C. Lin,[2] A. Karim Hussain,[1] Saskia Maas,[3] Horng J. Lai,[4] Harold Linnartz,[5] Thomas J. T. P. van den Berg,[6] Daniela C. F. Salvatori,[3] Gregorius P. M. Luyten,[1] and Martine J. Jager[1]

[1]Department of Ophthalmology, Leiden University Medical Center (LUMC), Leiden, The Netherlands
[2]Department of Research, Body Organ Biomedical Corporation, Taipei, Taiwan, Republic of China
[3]Central Animal Facility, Leiden University Medical Center (LUMC), Leiden, The Netherlands
[4]Department of Research, Aeon Astron Europe B.V., Leiden, The Netherlands
[5]Sackler Laboratory for Astrophysics, Leiden Observatory, Leiden University, Leiden, The Netherlands
[6]Netherlands Institute for Neuroscience, Royal Netherlands Academy of Arts and Sciences, Amsterdam, The Netherlands

PURPOSE. A fish scale–derived collagen matrix (FSCM) is proposed as an alternative for human donor corneal tissue. Light scatter and light transmission of the FSCM were measured and compared with human cornea, and its short-term biocompatibility was tested in a rat model.

METHODS. Light scatter was determined with a straylight measuring device, whereas light transmission was measured using a broadband absorption spectrometer. For evaluation of the biocompatibiliy, three approaches were used: the FSCM was implanted as an anterior lamellar keratoplasty (ALK), placed in an interlamellar corneal pocket (IL), and placed subconjunctivally (SC). Transparency, neovascularization, and epithelial damage were followed for 21 days. Morphology and cellular infiltration were assessed histologically.

RESULTS. The amount of scattered light was comparable to that seen in early cataract and the percentage of light transmission was similar to the transmission through the human cornea. Implantation of the FSCM as an ALK led to mild haziness only, not obscuring the pupil, despite the development of neovascularization around the sutures; IL placement led to a moderate haze, partly obscuring the pupil, and to (partial) melting of the anterior corneal lamella. The SC group exhibited local swelling and induration, which decreased over time. Histology showed a chronic inflammation varying from mild and moderate in the ALK and IL group, to severe in the SC group.

CONCLUSIONS. In spite of technical difficulties, it was feasible to use the FSCM for ALK, whereas IL placement led to melting of the anterior lamella. Further studies are necessary for better understanding of its immunogenicity. The light scatter and transmission data show that the first version of this FSCM is comparable to human cornea tissue in this respect.

Keywords: keratoprosthesis, artificial cornea, biocompatibility, transparency

C orneal disease is a major cause of blindness worldwide, second only to cataract. Globally, more than 10 million individuals are bilaterally blind due to corneal pathology and even more unilaterally.[1] Corneal transplantation is presently the only option to restore vision in these patients. Full-thickness corneal transplantation is one of the most successful forms of tissue transplantation and has been performed since 1905. One year after transplantation, the success rate is excellent in low-risk cases (avascular corneas). However, at longer follow-up, the overall acceptance of the grafts declines, particularly in high-risk cases.[2–5] The worldwide demand for human donor corneas, however, exceeds the world's supply, especially in developing countries.[6] Artificial corneal substitutes have emerged to counter this shortage and overcome the disadvantages of human donor corneas, including immune rejection. These corneal substitutes range from completely synthetic prostheses, which primarily aim to restore the cornea's refractive function,[7,8] and tissue-engineered cell-based con-

structs,[9] to hydrogels and scaffolds that facilitate the regeneration of the host tissue.[10–12]

Although much progress has been realized, keratoprostheses have not reached widespread use.[8] At the moment, they are too expensive and complex for routine use in developing countries, where the need for implants is highest. Alternatively, biological explants are being developed and tissue-engineered corneal epithelial cell sheets have been successfully transplanted in patients.[13–15] As corneal pathology often extends beyond the epithelium and affects the corneal stroma as well, replacement of the corneal stroma is usually necessary. To replace the corneal stroma, a cell-based construct or polymer scaffold of sufficient thickness is needed.

Ideally, such a scaffold for corneal regeneration allows reepithelialization, endothelialization, and repopulation with interstitial cells and nerves, preferably all of the patient's own origin. However, human corneal endothelium hardly regenerates. For many corneal opacities without endothelial involvement, procedures that preserve the recipient's endothelium are

used, such as anterior lamellar keratoplasty (ALK) and deep ALK (DALK). These anterior keratoplasties result in much better graft survival than the full-thickness grafts in penetrating keratoplasty (PK).[16–18] The anterior lamellar approach is therefore a logical starting point for scaffold-based corneal regeneration. In 2010, this approach was studied with a biosynthetic implant in a phase I clinical trial with 10 patients. Corneal regeneration with restored vision and sensitivity was found after 24 months of follow-up,[19] proving potential of this concept. The biosynthetic implant was synthesized from human recombinant collagen type I, which is an elaborate and rather expensive procedure, and despite the claimed success in this study, no new trials have started so far. Collagen scaffolds that already exist in nature may reduce the cost of fabrication and promise a sufficient resource for clinical transplantation even in developing countries. A decellularized porcine corneal matrix as a xenographic scaffold for corneal regeneration has been studied for several years by several research groups, as it closely resembles the human corneal stromal organization.[12,20,21] Indeed, such porcine matrices may offer a relative inexpensive and widely available alternative to human donor corneas. Results from clinical trials are not yet available, but a first phase I clinical trial is currently running.[22] Collagen matrices that are even more widely available, easier to harvest, and at lower expense, therefore definitely offer an interesting alternative, and this is the topic of our study.

Here we present the results of a matrix made from naturally occurring collagen type I and obtained from scales of the tilapia fish. Tilapia (Oreochromis mossambicus) are farmed for consumption under controlled circumstances[23] and the specific size of the fish can be selected on harvesting. Their scales consist of parallel-arranged collagen fibers packed in layers oriented approximately 90 degrees,[24] mimicking the human corneal stroma. This scaffold supports the growth of corneal cells and is highly permeable for oxygen.[25] Moreover, collagen sponges fabricated from reconstituted collagen fibers from tilapia scales produce only rare inflammatory responses in vivo.[26]

To investigate the suitability of this fish scale–derived collagen matrix (FSCM) for use as an artificial cornea, the light-scatter and light-transmission properties were examined. Also, in vivo studies were performed, using the rat keratoplasty model, widely employed for corneal transplantation studies.[27] We investigated the short-term biocompatibility and handling of the FSCM in three different surgical rat transplantation models.

METHODS

Fish Scale–Derived Artificial Cornea

A ±250-μm-thick decellularized and decalcified fish scale–derived extracellular matrix (ECM), consisting of collagen type I, was used for implantation (7-mm diameter, 0.2–0.3 mm thickness, P09011001; Aeon Astron Europe, Leiden, The Netherlands) (Fig. 1).[25] In short, fresh tilapia scales were cleaned in distilled water and cellular components were removed using a four-step detergent and enzymatic extraction process as developed by Courtman et al.[28] Acetic acid was used to increase pore size and porosity and nitric acid to decalcify the fish scales. The decellularized and decalcified scales were rinsed with 70% ethanol and stored until use in sterilized PBS at 4°C.

Top Pattern, Light Scatter, and Transmission

Phase-contrast images (Axio Observer.A1; Carl Zeiss AG, Jena, Germany) were taken of the prepared fish scale–derived
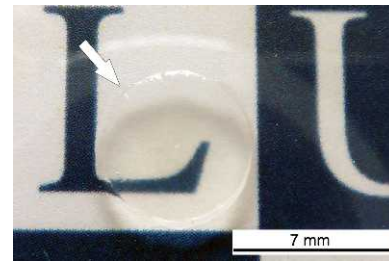

FIGURE 1. The fish scale–derived collagen matrix.

collagen scaffold and used to create a composition photograph in Adobe Photoshop (CS3 Extended, version 10.0; Adobe Systems Incorporated, San Jose, CA) to visualize the whole top surface. Scanning electron microscope images were taken of the cutting edge of the prepared FSCM and of the micro pattern on the top surface.

To measure forward light scatter, we chose a similar approach as is used clinically to assess the functional effect of forward light scatter in patients.[29] This way, the ex vivo results can directly be compared with clinical in vivo results. We applied a psychophysical technique known as “compensation comparison” and the outcome value is the straylight parameter “s.”[30] This technique is implemented in a commercial instrument (C-Quant; Oculus GmbH, Wetzlar, Germany) for clinical use, measuring the light scatter between 5 and 10 degrees, which has proved representative for the total amount of straylight (light scatter ≥ 1). We used this instrument, with a slight adaption, to assess forward light scatter from physical samples.[31] In short, two stimuli of the compensation comparison method, straylight flicker and comparison flicker, are presented to and compared by the subject simultaneously. To exclude the influence of light scatter provoked by the observer’s eye and to measure only the light scatter caused by the matrix, the straylight flicker source itself was shielded in such a way that it illuminated only the tested sample.[31] Three FSCMs (P11251101; 8.0 ± 0.8 mm [diameter], 0.25–0.35 mm [thickness]) were put on a test glass, one drop of PBS was used to prevent dehydration, and a cover glass was put on top. A black, opaque disk, with a central hole of 6.5-mm diameter, was mounted over the test glass, leaving only the FSCM visible. The test glass, with the FSCM and black opaque disk, was put in the ocular of the C-Quant device to measure the light scatter. Three measurements per FSCM were performed. A holder containing PBS without an FSCM acted as a control experiment.

To measure light transmission, three FSCMs (P11251101; 8.0 ± 0.8 mm [diameter], 0.25–0.35 mm [thickness]), placed in a sample holder and kept hydrated with PBS, were studied by a broadband absorption spectrometer, covering the visible and near infrared spectrum with a spectral resolution of 0.55 nm. Details are available from Bouwman et al.[32] The setup comprised a light source (LOT Oriel Xe-arc; 300-μm filament; LOT-QuantumDesign GmbH, Darmstadt, Germany) and spectrometer (Andor Shamrock SR-303i; Andor Technology PLC, Belfast, UK). The light source emitted white light with a homogeneous intensity pattern in the 200- to 760-nm region, fully covering the wavelength domain relevant to the human eye. This light was guided via a diaphragm through the center of the FSCM, which was placed 15 cm from the 10-μm wide inlet of the spectrometer. The sensor of the spectrometer measured light only in the horizontal plane. The maximum angle at which light could enter the spectrometer was 0.004 degrees. The spectrometer measured the direct light transmission, as straylight is defined as light being scattered at 1 or more degrees. All measurements were taken relative to

atmospheric air and normalized for background light. Normalization and measurement of transmission values for empty space were performed directly before each individual measurement. A holder containing only PBS was used to correct for light absorption or scatter caused by the holder itself. The light transmission of the visible spectrum was measured in steps of 0.56-nm wavelength and compared with the total light transmission of the human cornea, using the formula of van den Berg and Tan.[33]

Suturing

Two human donor eyes, obtained from the Euro Cornea Bank (Beverwijk, The Netherlands), were used to test the suturability of the scaffolds with nylon 10/0 sutures (nr. 8065 198001; Alcon B.V., Gorinchem, The Netherlands). In short, two FSCMs of 6-mm diameter were sutured into human corneas, 1 day postmortem, by placing 12 interrupted sutures in one case and continuous suture in the other, including knotting and burial of the knots. Severity of tearing due to the suturing was observed.

Animals

Eighteen male Fischer 344/DuCrl albino rats (Charles River Laboratory, L'Arbresle Cedex, France), each weighing between 280 and 336 g, were used for ocular implantation with permission of the Animal Ethics Committee of the Leiden University Medical Center. All animals were treated in accordance with the ARVO Statement for Use of Animals in Ophthalmic and Vision Research. They were given 1 week to acclimatize.

Implantation

The rats were divided into three groups of six animals, and in order to determine biocompatibility, scaffolds were placed in the anterior eye. In the first group, the FSCM, with the pattern on top, was placed as an ALK. In the second group, the FSCM was placed in an intralamellar pocket (IL), and in the last group it was inserted subconjunctivally (SC). The rats were anesthetized with isoflurane, with the addition of a topical drop of oxybuprocain and a subconjunctival injection of 20 μL bupivacain. Prior to implantation, the FSCM was soaked for 5 minutes in antibiotics (polyspectran containing gramicidine, neomycine, and polymyxine B).

ALK was performed by trephination of the right eye using a 3-mm trephine. The anterior tissue was removed using an air bubble, lamellar dissector, and scissors. The FSCM was cut to a diameter of 3.2 mm, inserted, and attached with eight nylon 10/0 sutures (nr. 8065 198001; Alcon B.V.). The surface of the FSCM was carefully leveled to line up with the native epithelium.

For the IL group, a nonpenetrating incision was made with a 15° stab knife and a pocket was created using an air bubble and a lamellar dissector. An FSCM with a diameter of 2.7 mm was inserted and the pocket was closed with two 10/0 nylon sutures.

SC implantation was performed by making an incision with a 15° stab knife. A blunt spatula was used to create a subconjunctival pocket, into which an FSCM with a diameter of 2.7 mm was inserted; the pocket was closed with two 10/0 nylon sutures.

Dehydration of the eye during surgery was prevented by regular wetting of the eye with special eye washings (balanced salt solution, 907553; Pharmacy LUMC, Leiden, The Netherlands). Directly after surgery, 1% chloramphenicol ointment (Chloramphenicol-POS 1%, 10 mg/g; Ursapharm Benelux B.V.,

Helmond, The Netherlands) was applied. In all cases, the unoperated left eye served as a control and was kept hydrated with gel (Vidisic Carbogel, carbomer 2 mg/g; Tramedico B.V., Weesp, The Netherlands) to prevent dryness during surgery.

In Vivo Observation

The animals were observed in the 3 weeks following implantation. Ocular drops with corticosteroids and antibiotics (Tobradex, containing dexamethasone and tobramycine; Alcon Cusi SA, Barcelona, Spain) were applied in the ALK and IL groups, once daily during the first week and every other day during the second week. All drops were stopped at the 2-week follow-up. The SC group did not receive any drops postoperatively.

At 2, 7, 13, and 21 days after implantation, all animals were examined with a microscope to judge neovascularization, transparency, and clinical signs of inflammation, such as conjunctival redness or purulent secretion. Corneal neovascularization was numerically scored from 0 to 5, with 0 = no vessels, 1 = growth of vessels at the limbus, 2 = vessels reaching the sutures/FSCM, 3 = vessels present underneath the FSCM, 4 = vessels entering the FSCM, and 5 = vessels present throughout the whole FSCM. Transparency of the cornea was assessed using a grading scale as previously used by Hackett et al.,[34] with 0 = transparent, 1 = a mild haze not obscuring the pupil, 2 = a moderate haze partially obscuring the pupil, and 3 = an opaque area totally obscuring the pupil.

Histopathological Evaluation

After euthanizing the 16 rats with carbon dioxide, the eyes were enucleated and fixated with Davidson solution (composed of glacial acetic acid, ethyl alcohol, and buffered formalin) and then dehydrated and embedded in paraffin. Sections were cut on a microtome (Leica RM2165; Leica Microsystems GmbH, Wetzlar, Germany) at 5 μm and stained with hematoxylin and eosin (HE) for histological examination. All eyes were analyzed for the organization of the epithelium, stroma, and endothelium, and scored semiquantitatively for infiltration of immune cells and ingrowth of corneal cells into the FSCM. The immune infiltrate was characterized based on morphology.

Statistical Analysis

All statistical analyses were performed using a statistical software program (SPSS for Microsoft Windows, version 17.0.2; IBM SPSS Statistics, IBM Corporation, Chicago, IL). The χ^2 trend test was used for assessing differences between the groups regarding corneal neovascularization and opacification, and leukocyte infiltration. Statistical significance was assumed for resulting P values less than 0.05.

RESULTS

Top Pattern, Light Scatter, and Light Transmission

The whole top surface of the FSCM was visualized with a composed phase-contrast image. The micro pattern on top of the FSCM differed per area, with roughly one quarter having a spider-web appearance with micro ridges and channels, two quarters exhibiting circular running ridges and channels, but without intersecting lines, and the last quarter consisting of spikes (Fig. 2a). SEM images of the FSCM confirmed these findings (Figs. 2b–d). The micro ridges were wavelike in shape, ±5.7 μm high, and ±3.4 μm wide. The channels in between were indeed ±30 μm wide (Fig. 3).[25]
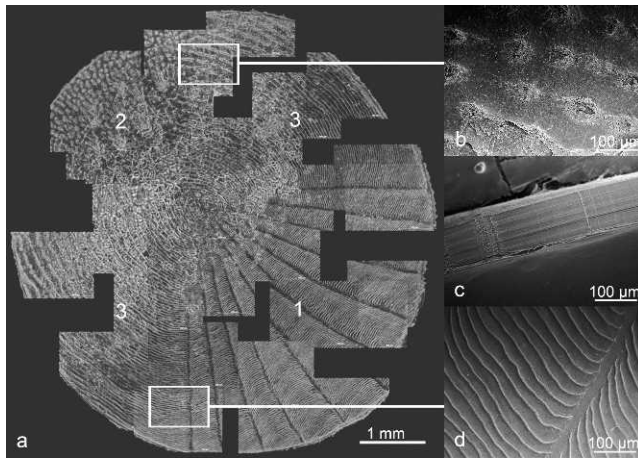
FIGURE 2. Composition of several phase-contrast images showing the distribution of the micro pattern with the spokes and interconnecting channels in one quadrant (**a-1**), the spikes in the opposite quarter (**a-2**), and the circular running lines in the area (**a-3**) between those two quadrants. Detailed SEM-images depict the transitional area between the circular lines and spikes (**b**), between the lines and spokes (**d**), and a cross section showing the multiple layers (**c**).

The amount of straylight was measured for three FSCMs using the compensation comparison method. Log values for forward light scatter caused by the holding device were beyond the lowest measurable value for the C-Quant device (log [s] < 0.40) and were considered to be negligible. The mean light scatter of the three FSCMs was log (s) = 1.62. All results are listed in Table 1.

Direct light transmission of the visible spectrum was measured on another three FSCMs. The mean direct light transmission of the three measured FSCMs, corrected for reduction of light transmission caused by the PBS-filled holder, amounted to 89%, 97%, and 85% and showed corresponding curved graphs (Fig. 4a). The three measurements were grouped and compared with the total light-transmission curve of the human cornea (Fig. 4b). The human corneal light-
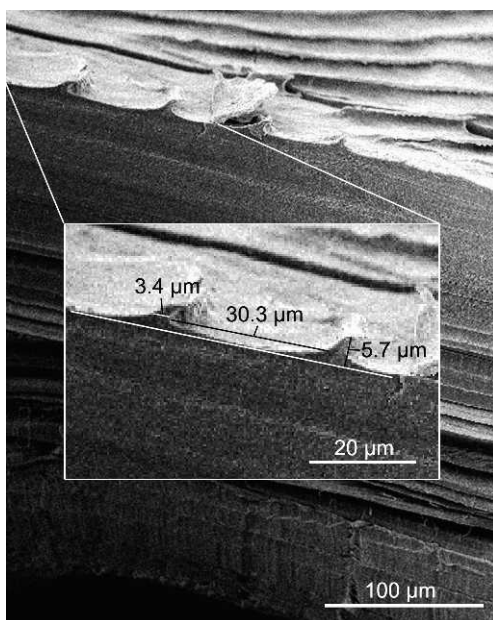

FIGURE 3. Cross section of the FSCM showing the dimensions of the circular running ridges on the surface.

TABLE 1. Forward Light Scatter Results in Log(s) With Oculus (C-Quant)

Measurements	First	Second	Third	Mean
FSCM 1	1.50	1.53	1.46	1.50
FSCM 2	1.66	1.69	1.74	1.70
FSCM 3	1.62	1.65	1.63	1.63
Mean				1.62

transmission values were within the SEM of the FSCM light-transmission values. The mean direct light transmission of the FSCM was 90%, whereas the total light transmission of the human cornea was 91%.[33]

Suturing

Suturing tests with the two FSCMs revealed in both methods no tearing at the suture points and the knots could be buried. On bringing in the suture needle, confined cracking occurred. Micro-shearing at the suture points of the FSCM (and not of the human cornea) was observed on tightening some of the knots.

Short-Term Biocompatibility

To determine the scaffold's biocompatibility, FSCMs were placed in the cornea as ALKs, placed intracorneally (intralamellar pockets) and placed subconjunctivally.

One week following transplantation, all six rats that underwent ALK had a clear and quiet cornea, with minimal neovascularization in maximally one quadrant. After 2 weeks, the scaffolds remained in place, while neovascularization was reaching the FSCM. In five cases, a mild haze at the edge of the FSCM, not obscuring the pupil, was observed, and in the sixth animal, the haze partially obscured the pupil. Sutures started to loosen slightly in all cases. At the 3-week end point, the neovascularization extended underneath the FSCM with vessels aimed at the sutures, but not penetrating the FSCM. The haze increased slightly, not obscuring the pupil. Gradual loosening of the sutures resulted in loss of the FSCM in two cases at day 18 and 21, as the rats were allowed to move freely and touch their eyes. These cases were excluded from further analysis.

During follow-up, the eyes were stained with fluorescein to analyze epithelialization. In the ALK group, the total area of the FSCM stained positively, indicating the absence of reepithelialization of the FSCM surface after 3 weeks.

Implantation in an intralamellar pocket was performed in six rats. The results were less uniform than found for the ALK implants. After 1 week, two cases showed no haze, two cases exhibited a mild haze that did not obscure the pupil, and the remaining two rats showed a moderate haze, partially obscuring the pupil. In four cases, blood vessels approached the sutures located near the limbus. All sutures were removed after 1 week. After 2 weeks, superficial vessels reached the FSCM. The amount of haze remained stable, while some melting of the anterior lamella in front of the FSCM was noticed in five animals. Two animals were killed at 13 and 19 days postimplantation due to too much weight loss. When the 3-week end point was reached, blood vessels reached the FSCM in the remaining four animals, with some vessels starting to invade the over- or underlying stroma. Vessels did not invade the matrix and were less dense than in the ALK group.

After 3 weeks, the corneal haziness had slightly increased in three animals, ranging from a mild haze to an opaque area totally obscuring the pupil. In one case, however, the neovascularization had diminished and remained present only in the limbal area and a moderate corneal haze was observed.
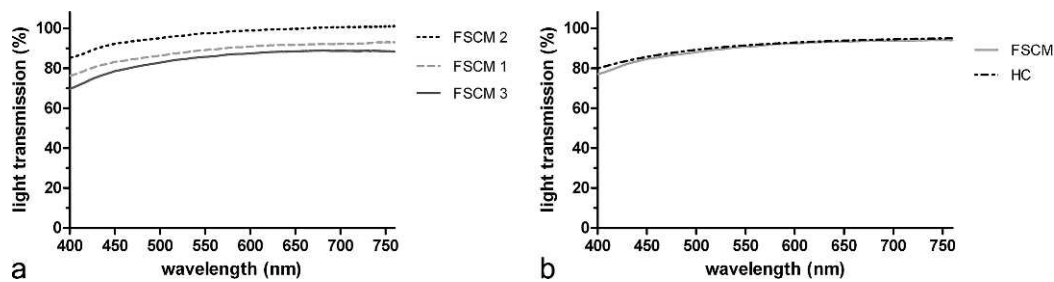
FIGURE 4. Direct light-transmission curves for the visible spectrum of three FSCMs (**a**), and the mean direct light transmission of the FSCM compared with the total light transmission of the human cornea (**b**). HC, human cornea.

Corneal fluorescein staining revealed melted areas of the anterior lamella of variable size in all four remaining cases.

The six rats receiving an SC implant showed slight SC swelling postoperatively at the implantation site. The swelling disappeared after 2 weeks in four rats and lasted until the end point in two rats. Local conjunctival hyperemia was present at a low degree until the end point. Sutures were not removed, as within 1 week the sutures were overgrown by the conjunctiva and removal without damaging the surrounding area proved to be difficult.

Overall

Except for the two cases mentioned, all implanted animals were in good health, kept their weight, and showed no symptoms of any ocular infection or noticeable irritation. The FSCM flattened the recipient rat cornea due to a curvature disassociation. End point neovascularization and opacification (Figs. 5a, 5b) did not differ significantly ($P = 0.46$ and $P = 0.19$, respectively) between the ALK and IL groups. Typical cases of each implantation model are depicted in Figure 6. An overview of in vivo and histological characteristics is given in Table 2.

Histopathological Evaluation

To visualize the clinically observed changes with histology, sections of the four scaffold-containing corneas in the ALK group were cut, stained with HE, and compared with the control lateral eye (Figs. 7a, 7b). HE staining showed mild corneal edema with blood vessels and infiltrating leukocytes in the stroma around the sutures and at a lower degree under the FSCM (Figs. 7c, 7d). A few leukocytes were seen within the FSCM. The leukocytes showed a typically chronic inflammatory reaction with mainly macrophages and lymphocytes and some neutrophils. Epithelial downgrowth occurred in all cases at the border of the FSCM. At the location of the sutures and at

the border of the FSCM, the epithelium showed hyperplasia and metaplasia.

HE staining of the four cases of the IL group showed infiltration of immune cells, which consisted of the typical mixture with macrophages, lymphocytes, and some neutrophils. A few leukocytes were found within the FSCM (Fig. 7e). Local edema, metaplasia, and necrotic cells of the epithelium overlying the FSCM were observed in three of the four cases (Figs. 7e, 7f). However, one of the implants had no leukocytes or blood vessels infiltrating the stroma (Fig. 7f) and the other only a few (not shown). This corresponded with the in vivo observations (Figs. 6f–j). Infiltration of immune cells was not significantly different between the ALK and IL groups ($P = 0.57$) (Fig. 8).

The SC implants were completely surrounded by leukocytes in all six cases, with several leukocytes invading the FSCM. The leukocyte infiltration was limited to the adjacent surrounding tissue, again representing chronic inflammation. The SC group showed significantly more infiltration than the ALK group ($P = 0.04$) and the IL group ($P = 0.02$) (Fig. 8). The tissue surrounding the implant showed edema (Figs. 7g, 7h). Compared with nonoperated control eyes, more vessels were present.

Discussion

Pattern and Light Scatter and Transmission

The composed phase-contrast image of the FSCM shows that the pattern that contains the micro channels covers only a quarter and not the full surface. This is in accordance with the natural pattern of the so-called ctenoid fish scales.[35] Nevertheless, this nonhomogeneity of the pattern does not prevent corneal stromal cells from populating the scaffold's surface, and is perhaps even stimulating cell spread.[25] The circular running ridges had a height and width much larger than the visible wavelengths, thereby provoking light scatter. This is in
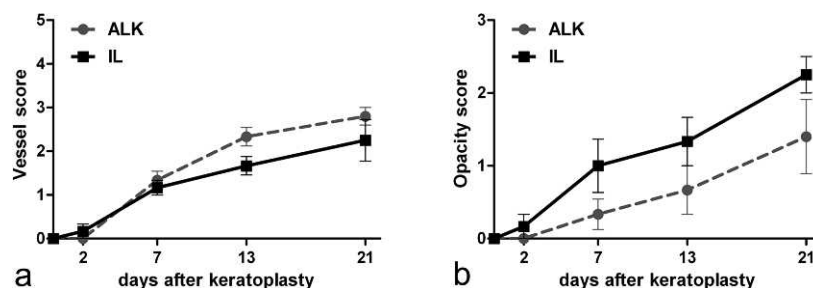

FIGURE 5. Scoring of corneal neovascularization (**a**) and opacification (**b**) at different time points during follow-up of the ALK and IL groups. Vessel score and opacity score did not differ significantly at the 21-day end point (respectively $P = 0.46$ and $P = 0.19$; χ^2 trend test). Greatest difference of vessel score between the two groups at day 13 was not significant either ($P = 0.14$). *Error bars* represent SEM. Vessel score: 0 = none; 1 = at limbus; 2 = reaching sutures /FSCM; 3 = under FSCM; 4 = entering FSCM; 5 = whole FSCM. Opacity score: 0 = transparent; 1 = mild haze, not obscuring the pupil; 2 = moderate haze partially obscuring the pupil; 3 = opaque area totally obscuring the pupil.
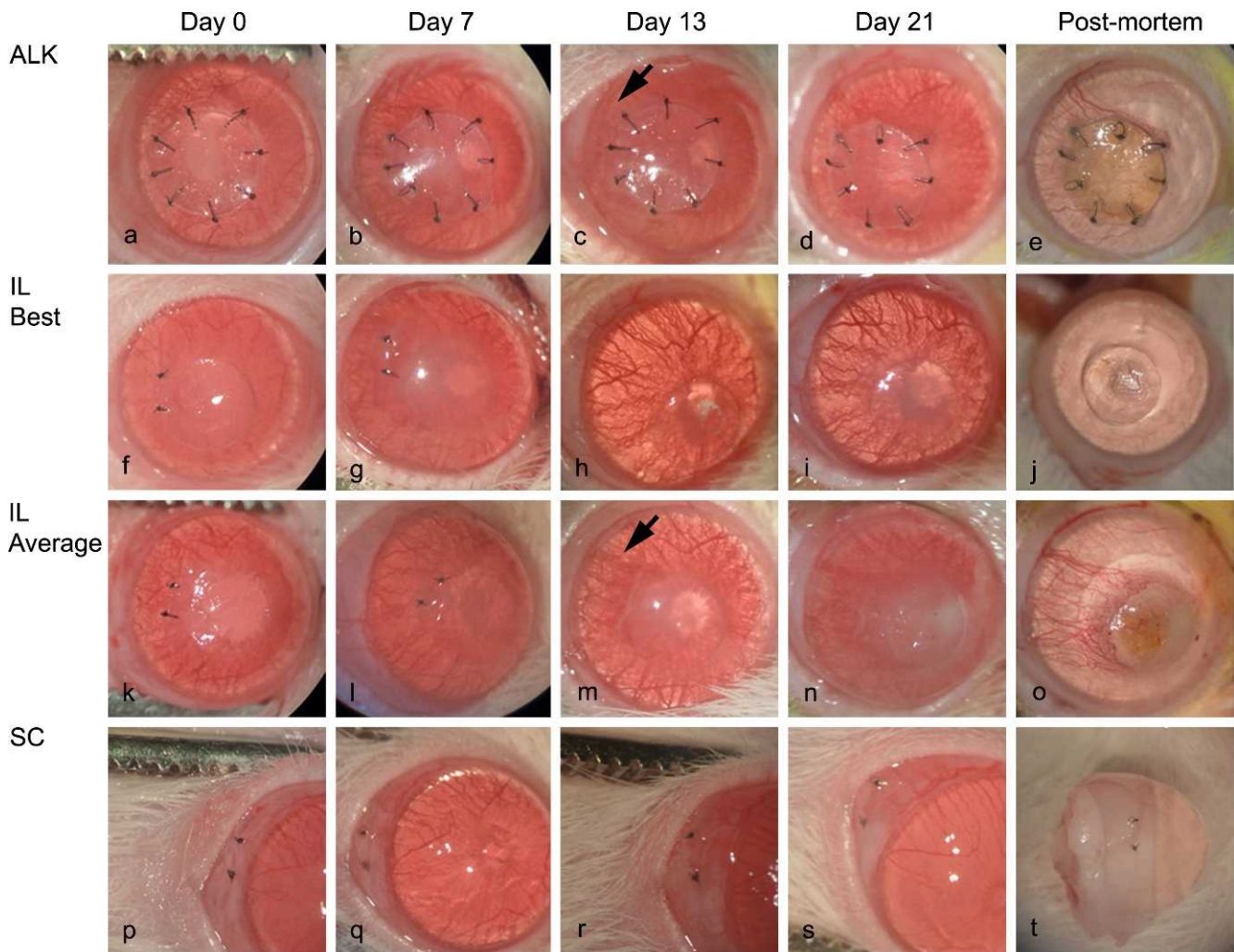
Investigative Ophthalmology & Visual Science

Figure 6. Typical cases of each implantation model are shown. The IL group has been separated in best result and average result, due to high variability. All groups showed good transparency of the corneal implants on microscopic examination directly postoperatively (*first column*: [a, f, k, p]) and up to 7 days (*second column*: [b, g, l, q]). Neovascularization and opacification were visible at 13 days (*third column*: [c, h, m, r]) and gradually increased until day 21 (*fourth column*: [d, i, n, s]). Neovascularization is seen even more clearly postmortem (*last column*: [e, j, o, t]).

accordance with the observations that the pattern was clearly visible under the phase-contrast microscope. The latter visualizes differences in refraction, which may cause light scattering.

The FSCM had a forward light scattering of log(s) = 1.62, comparable to the amount of scattering caused by early cataract.[30,36] The direct light transmission was 90%. Even though this value reflects the direct transmission and not the total light transmission, which includes forward-scattered light as well, it is very close to the total light transmission of 91% found for the human cornea. The light-transmission curves of the FSCM and human cornea are also very similar in shape, indicating corresponding values of Rayleigh scatter (i.e., light scatter caused by particles much smaller than the wavelength of light such as molecules). The displacement along the y-axis of the light-transmission curves for the different FSCMs can be attributed to a wavelength-independent scatter, plausibly caused by the micro pattern that roughens the surface of the FSCM with ridges larger in size than the wavelength of visible light. Although special care was taken for optimum position, it could not be prohibited that each FSCM was slightly differently positioned relative to the spectrometer and therefore caused different amounts of scatter. Removal of the micro pattern

from the FSCM surface will improve light transmission and especially light-scatter values, which in turn will result in better visual acuity when implanted.

Suturing

The suturing test demonstrated that the FSCM can be sutured successfully into the cornea, when handled with care. The scaffold was brisker and had less mechanical strength than the human cornea (or rat cornea), indicated by the confined cracking and shearing. Increasing the elasticity and strength likely will improve the ease of handling and this may be needed to make the FSCM applicable for full-thickness transplantation in humans.

In Vivo Biocompatibility

The rat keratoplasty model has been used to study corneal transplantation for more than 25 years.[27] Our findings of this first in vivo study with the FSCM correspond to the results seen with allogeneic corneal transplantations in rats.[37–39] All corneal implants showed good acceptance up to 1 week postoperatively with neovascularization limited to one quadrant of the limbal rim, no opacity at all in the ALK group, and mild opacity in the IL group. After 3 weeks, neovascularization had

TABLE 2. Overview of In Vivo and Histological Characteristics

	Follow-Up, d	FSCM Lost	Corneal Vessel Score, d 21	Opacity Score, d 21	Excluded on Histology	Corneal Epith. Atrophy	Corneal Epith. Hyperplasty	Corneal Epith. Metaplasia	Corneal Epith. Downgrowth	Leukocyte Infiltration
ALK 1	21	N	2	1	N	–	+++	+	Y	++
ALK 2	21	N	3	3	N	+	++	+	Y	+++
ALK 3	21	N	3	1	N	+	++	+	Y	+
ALK 4	21	Y	3	0	N	N/A	N/A	N/A	N/A	N/A
ALK 5	21	N	3	2	N	+	++	++	Y	++
ALK 6	18	Y	–	–	Y	N/A	N/A	N/A	N/A	N/A
IL 1	13	Y	–	–	Y	N/A	N/A	N/A	N/A	N/A
IL 2	13	N	–	–	Y	N/A	N/A	N/A	N/A	N/A
IL 3	21	N	3	2	N	+	++	+	N	++
IL 4	21	N	2	2	N	++	++	+	N	–/+
IL 5	21	N	3	3	N	+	+	+	N	++
IL 6	21	N	1	2	N	++	+	++	N	–
SC 1	21	N	0	0	N	N/A	N/A	N/A	N/A	+++
SC 2	21	N	0	0	N	N/A	N/A	N/A	N/A	+++
SC 3	21	N	0	0	N	N/A	N/A	N/A	N/A	+++
SC 4	21	N	0	0	N	N/A	N/A	N/A	N/A	+++
SC 5	21	N	0	0	N	N/A	N/A	N/A	N/A	+++
SC 6	21	N	0	0	N	N/A	N/A	N/A	N/A	+++

Epith., epithelial; N, no; N/A, not applicable; Y, yes; – = absent, + = mild, ++ = moderate, +++ = severe.
Corneal vessel score: 0 = none; 1 = at the limbus; 2 = reaching sutures/FSCM; 3 = under FSCM; 4 = in FSCM; 5 = whole FSCM.
Opacity score: 0 = transparent; 1 = mild haze, not obscuring the pupil; 2 = moderate haze partially obscuring pupil; 3 = opaque area totally obscuring pupil.

increased until it reached the FSCM and sutures, but vessels failed to penetrate the FSCM. The opacity gradually increased to a mild haze (stage 1) in the ALK group and a moderate haze (stage 2) in the IL group. Total opacification (stage 3) of the FSCM, indicative for a complete rejection, was observed in only one animal of the IL group. It is important to note that in humans with a nonvascularized cornea, a non-HLA–matched allogeneic corneal transplantation has a high acceptance rate, whereas in rats, this situation leads to rejection after 5 to 15 days.[37–39] A rejected graft is recognized by complete corneal opacification and infiltrating T cells on histology. The main finding of this study on the short-term biocompatibility and handling of the FSCM to obtain a first impression of its use as a replacement of human donor material, is that the FSCM may have potential for corneal applications in humans.

The local abnormalities that occurred in the corneal epithelium are largely explained by mechanical irritation induced by the FSCM. The edges were standing out due to a relative mismatch in curve and thickness and insufficient elasticity. This led to compression of the overlaying stroma and epithelium and created a tear meniscus in the IL group. These characteristics also explain the development of epithelial downgrowth that occurred in the ALK group. The dense structure and thickness of the FSCM may have put pressure on the remaining corneal tissue in the IL group, prohibiting adequate flow of nutrients from the anterior chamber toward the overlaying anterior cornea. This mechanism, together with a too shallow implantation, is thought to be responsible for the observed melting. Histology confirmed that the cases with lesser melting were indeed implanted at a greater depth.

The amount of neovascularization was comparable to that seen in allogeneic corneal transplantations in rats[38,40] and provoked by the sutures.[41] This explains the higher degree of neovascularization in the ALK group, in which more sutures were used and not removed, in contrast to the IL group, in which two sutures were used and removed after 2 weeks. In both groups, vessels failed to invade the FSCM, perhaps due to

the fibril density of the FSCM or by yet to be identified antiangiogenic properties.

Corneal opacification, which indicates swelling or an ongoing immune reaction, reached levels compatible with a complete rejection in 2 of the 12 corneal implants. The observed opacification may be due to the mentioned mechanical irritation, which leads to corneal damage and subsequent leukocyte infiltration.

The infiltration of leukocytes was mild to moderate and consisted predominantly of macrophages, lymphocytes, and some neutrophils, indicative of a chronic immune reaction. The leukocytic infiltration was primarily aimed at the sutures in the ALK group and surrounded the scaffold in the SC group and partly in the IL group. The SC group showed the presence of fibroblasts aligned around the scaffold, similar to a mild foreign body reaction.[42] It is unlikely that this infiltration and swelling is caused by pathogens present on the FSCM prior to implantation, as FSCMs from the same batch were tested and found to be negative for bacteria and fungi. Furthermore, a more severe reaction is expected in case of infection. Type 1 collagen of fish is similar to that of humans[43] and reconstituted tilapia collagen sponges caused only rare inflammatory responses.[26] Still, the collagen of the FSCM or residues of chemicals used for decellularization and decalcification could have provoked the immune response. A strong argument to support the notion that the inflammation was due to surgical trauma and mechanical irritation is the complete absence of inflammation in one case. If the inflammation had been due to a heterologous protein, one would have expected an immune response in all cases. The gradual tearing of the sutures through the FSCM, as noticed after 2 weeks, was aggravated by the outstanding edges and additional external mechanical forces caused by blinking and eye movements. Placing a contact lens or increasing the elasticity or curvature of the FSCM may offer a pathway to prevent this.[44] The increased cellular infiltration and swelling on the histology of the SC group is well explained by the less immune privilege of the conjunctiva compared with the cornea.
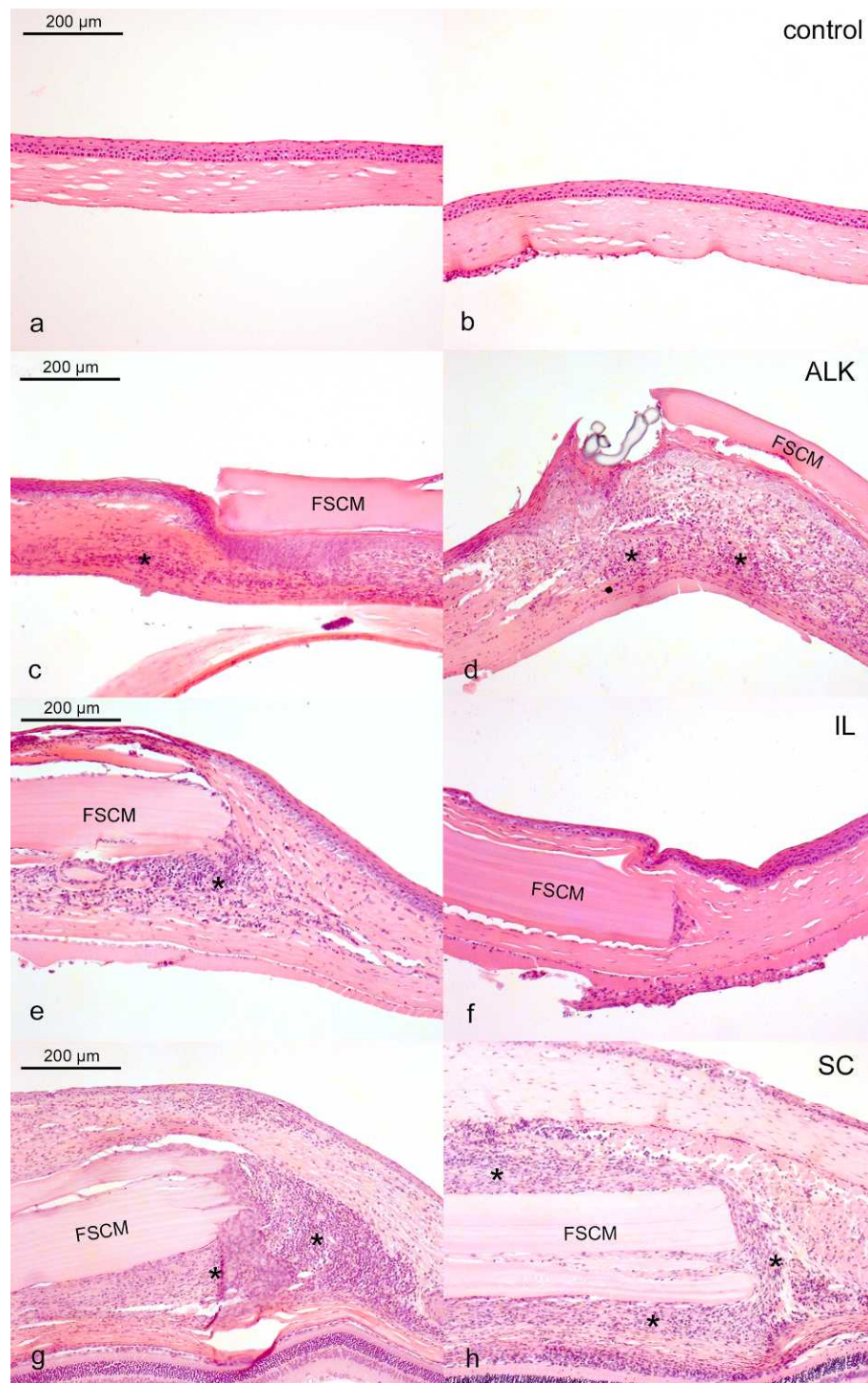
FIGURE 7. HE stainings. Examples of control corneas are shown (**a**, **b**). The ALK group had mild to moderate infiltration of leukocytes, epithelial hyper- and metaplasia, and epithelial downgrowth due to mismatch in shape (**c**, **d**). The IL group had a mild to moderate infiltration in two cases (**e**) and almost no infiltration in two other cases (**f**); all IL cases showed local atrophy and metaplasia of the epithelium (**e**, **f**). The SC group showed moderate infiltration (**g**, **h**), with fibrous capsule formation and some leukocytes infiltrating between the layers (**h**). *Leukocyte infiltration and concomitant edema.

Other collagen matrices used for corneal regeneration, such as the biosynthetic artificial cornea,[19] are already being used in clinical studies, following a decennium of preclinical research.[45] The novelty and advantage of the FSCMs are its wide availability, its low cost, and simple manufacturing process. However, we are at an early phase in our research, and working on overcoming technical challenges so as to develop a useful prototype.

CONCLUSION

This systemic study of the physical and biomedical short-term effects of the FSCM as corneal replacement, demonstrates its potential for future use. The availability of an easy obtainable and biocompatible FSCM can have a high impact on decreasing the shortage of donor corneas and make lifelong use of
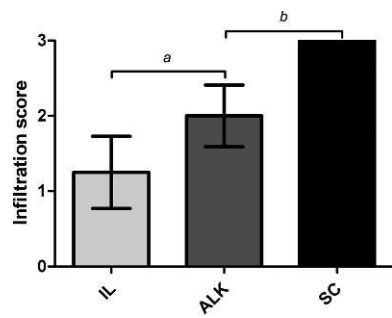
immunosuppressive medication redundant. The potential of this FSCM is demonstrated for the first time by an adequate light transmission, reasonable light-scattering values, and ability to be used in keratoplasty. Future studies with a curved and thinner FSCM are necessary to prevent mechanical irritation and increase the understanding of its immunogenicity. Long-term in vivo studies and studies on modified FSCMs, for instance with the top pattern removed, are needed to develop and optimize this readily available collagen matrix as an artificial cornea.

References

1. Whitcher JP, Srinivasan M, Upadhyay MP. Corneal blindness: a global perspective. *Bull World Health Organ*. 2001;79:214–221.

2. Williams KA, Roder D, Esterman A, Muehlberg SM, Coster DJ. Factors predictive of corneal graft survival. Report from the Australian Corneal Graft Registry. *Ophthalmology*. 1992;99:403–414.

3. Williams KA, Muehlberg SM, Lewis RF, Coster DJ. How successful is corneal transplantation? A report from the Australian Corneal Graft Register. *Eye (Lond)*. 1995;9:219–227.

4. Thompson RW Jr, Price MO, Bowers PJ, Price FW Jr. Long-term graft survival after penetrating keratoplasty. *Ophthalmology*. 2003;110:1396–1402.

5. Waldock A, Cook SD. Corneal transplantation: how successful are we? *Br J Ophthalmol*. 2000;84:813–815.

6. Hara H, Cooper DK. Xenotransplantation—the future of corneal transplantation? *Cornea*. 2011;30:371–378.

7. Myung D, Duhamel PE, Cochran JR, Noolandi J, Ta CN, Frank CW. Development of hydrogel-based keratoprostheses: a materials perspective. *Biotechnol Prog*. 2008;24:735–741.

8. Gomaa A, Comyn O, Liu C. Keratoprostheses in clinical practice—a review. *Clin Experiment Ophthalmol*. 2010;38:211–224.

9. Proulx S, d'Arc UJ, Carrier P, et al. Reconstruction of a human cornea by the self-assembly approach of tissue engineering using the three native cell types. *Mol Vis*. 2010;16:2192–2201.

10. McLaughlin CR, Acosta MC, Luna C, et al. Regeneration of functional nerves within full thickness collagen-phosphoryl-choline corneal substitute implants in guinea pigs. *Biomaterials*. 2010;31:2770–2778.

11. Fagerholm P, Lagali NS, Carlsson DJ, Merrett K, Griffith M. Corneal regeneration following implantation of a biomimetic tissue-engineered substitute. *Clin Transl Sci*. 2009;2:162–164.

12. Yoeruek E, Bayyoud T, Maurus C, et al. Reconstruction of corneal stroma with decellularized porcine xenografts in a rabbit model. *Acta Ophthalmol*. 2012;90:e206–e210.

13. Tseng SC, Prabhasawat P, Barton K, Gray T, Meller D. Amniotic membrane transplantation with or without limbal allografts for corneal surface reconstruction in patients with limbal stem cell deficiency. *Arch Ophthalmol*. 1998;116:431–441.

14. Meller D, Pauklin M, Thomasen H, Westekemper H, Steuhl KP. Amniotic membrane transplantation in the human eye. *Dtsch Arztebl Int*. 2011;108:243–248.

15. Koizumi N, Inatomi T, Suzuki T, Sotozono C, Kinoshita S. Cultivated corneal epithelial stem cell transplantation in ocular surface disorders. *Ophthalmology*. 2001;108:1569–1574.

16. Sarnicola V, Toro P, Sarnicola C, Sarnicola E, Ruggiero A. Long-term graft survival in deep anterior lamellar keratoplasty. *Cornea*. 2012; 31:621–626.

17. Reinhart WJ, Musch DC, Jacobs DS, Lee WB, Kaufman SC, Shtein RM. Deep anterior lamellar keratoplasty as an alternative to penetrating keratoplasty: a report by the American Academy of Ophthalmology. *Ophthalmology*. 2011;118:209–218.

18. Borderie VM, Sandali O, Bullet J, Gaujoux T, Touzeau O, Laroche L. Long-term results of deep anterior lamellar versus penetrating keratoplasty. *Ophthalmology*. 2012;119:249–255.

19. Fagerholm P, Lagali NS, Merrett K, et al. A biosynthetic alternative to human donor tissue for inducing corneal regeneration: 24-month follow-up of a phase 1 clinical study. *Sci Transl Med*. 2010;2:46ra61.

20. Zhou Y, Wu Z, Ge J, et al. Development and characterization of acellular porcine corneal matrix using sodium dodecylsulfate. *Cornea*. 2011;30:73–82.

21. Du L, Wu X. Development and characterization of a full-thickness acellular porcine cornea matrix for tissue engineering. *Artif Organs*. 2011;35:691–705.

22. Liu J. Xiamen University. Phase I Study of xenogenic keratoplasty from porcine cornea in the treatment of infectious corneal ulcer. Bethesda, MD: National Library of Medicine; 2013. Available at: http://www.clinicaltrials.gov/ct2/show/NCT01443559. Accessed January 15, 2013.

23. Chen MH, Li YH, Chang Y, et al. Co-induction of hepatic IGF-I and progranulin mRNA by growth hormone in tilapia, *Oreochromis mossambiccus*. *Gen Comp Endocrinol*. 2007;150:212–218.

24. Okuda M, Ogawa N, Takeguchi M, et al. Minerals and aligned collagen fibrils in tilapia fish scales: structural analysis using dark-field and energy-filtered transmission electron microscopy and electron tomography. *Microsc Microanal*. 2011;17:788–798.

25. Lin CC, Ritch R, Lin SM, et al. A new fish scale-derived scaffold for corneal regeneration. *Eur Cell Mater*. 2010;19:50–57.

26. Sugiura H, Yunoki S, Kondo E, Ikoma T, Tanaka J, Yasuda K. In vivo biological responses and bioresorption of tilapia scale collagen as a potential biomaterial. *J Biomater Sci Polym Ed*. 2009;20:1353–1368.

27. Williams KA, Coster DJ. Penetrating corneal transplantation in the inbred rat: a new model. *Invest Ophthalmol Vis Sci*. 1985; 26:23–30.

28. Courtman DW, Pereira CA, Kashef V, McComb D, Lee JM, Wilson GJ. Development of a pericardial acellular matrix biomaterial: biochemical and mechanical effects of cell extraction. *J Biomed Mater Res*. 1994;28:655–666.

29. Coppens JE, Franssen L, van den Berg TJ. Reliability of the compensation comparison method for measuring retinal stray light studied using Monte-Carlo simulations. *J Biomed Opt*. 2006;11:054010.

30. van den Berg TJ, Franssen L, Kruijt B, Coppens JE. History of ocular straylight measurement: a review. *Z Med Phys*. 2013;23: 6–20.

31. van den Berg TJ, Franssen L, Coppens JE. Straylight in the human eye: testing objectivity and optical character of the psychophysical measurement. *Ophthalmic Physiol Opt*. 2009; 29:345–350.

32. Bouwman J, Paardekoper DM, Cuppen HM, Linnartz H, Allamandola LJ. Real-time optical spectroscopy of vauum ultraviolet irradiate pyrene: H2O interstellar ice. *Astrophys J*. 2009;700:56–62.

33. van den Berg TJ, Tan KE. Light transmittance of the human cornea from 320 to 700 nm for different ages. *Vision Res*. 1994;34:1453–1456.

34. Hackett JM, Lagali N, Merrett K, et al. Biosynthetic corneal implants for replacement of pathologic corneal tissue: performance in a controlled rabbit alkali burn model. *Invest Ophthalmol Vis Sci*. 2011;52:651–657.

35. Sire JY, Arnulf I. Structure and development of the ctenial spines on the scales of a teleost fish, the cichlid *Cichlasama nigrofasciatum*. *Acta Zoologica*. 2000;81:139–158.

36. Nischler C, Michael R, Wintersteller C, et al. Cataract and pseudophakia in elderly European drivers. *Eur J Ophthalmol*. 2010;20:892–901.

37. Birnbaum F, Schwartzkopff J, Scholz C, Reinhard T. Topical pimecrolimus does not prolong clear graft survival in a rat keratoplasty model. *Graefes Arch Clin Exp Ophthalmol*. 2007; 245:1717–1721.

38. Rocher N, Behar-Cohen F, Pournaras JA, et al. Effects of rat anti-VEGF antibody in a rat model of corneal graft rejection by topical and subconjunctival routes. *Mol Vis*. 2011;17:104–112.

39. Hosseini A, Lattanzio FA Jr, Samudre SS, Disandro G, Sheppard JD Jr, Williams PB. Efficacy of a phosphorodiamidate morpholino oligomer antisense compound in the inhibition of corneal transplant rejection in a rat cornea transplant model. *J Ocul Pharmacol Ther*. 2012;28:194–201.

40. Schwartzkopff J, Bredow L, Mahlenbrey S, Boehringer D, Reinhard T. Regeneration of corneal endothelium following complete endothelial cell loss in rat keratoplasty. *Mol Vis*. 2010;16:2368–2375.

41. Li Z, Yao L, Li J, et al. Celastrol nanoparticles inhibit corneal neovascularization induced by suturing in rats. *Int J Nanomedicine*. 2012;7:1163–1173.

42. Vaisman B, Motiei M, Nyska A, Domb AJ. Biocompatibility and safety evaluation of a ricinoleic acid-based poly(ester-anhydride) copolymer after implantation in rats. *J Biomed Mater Res A*. 2010;92:419–431.

43. Bolboaca SD, Jantschi L. *Amino Acids Sequences Analysis on Collagen*. Vol. 63–64. Waltham, MA: Academic Press; 2007; 311–316.

44. Merrett K, Liu W, Mitra D, et al. Synthetic neoglycopolymer-recombinant human collagen hybrids as biomimetic cross-linking agents in corneal tissue engineering. *Biomaterials*. 2009;30:5403–5408.

45. Merrett K, Griffith CM, Deslandes Y, Pleizier G, Sheardown H. Adhesion of corneal epithelial cells to cell adhesion peptide modified pHEMA surfaces. *J Biomater Sci Polym Ed*. 2001;12: 647–671.